sciendo

Nova Biotechnol Chim (2019) 18(2): 166-178
DOI: 10.2478/nbec-2019-0019

Nova Biotechnologica *et* Chimica

Treatment and remediation by the stabilization/solidification process based on hydraulic binders of soil contaminated by heavy metals

Rachid Sahnoune and Karim Moussaceb✉

Laboratoire de Technologie des Matériaux et de Génie des Procédés (LTMGP), Faculté de Technologie, Université A/MIRA Bejaia, Route Targa-Ouzemour, Bejaia 06000, Algeria

Article info

Article history:
Received: 21st May 2019
Accepted: 20th November 2019

Keywords:
Contamination
Heavy Metals
Hydraulic Binders
Remediation
Soils
Stabilization/Solidification

Abstract

Nature and the environment are affected by various human industrial and/or urban discharges. Remediation for this problem requires first and foremost an in-depth analysis and an overall characterization of the intrinsic properties of the pollution-receiving environments. Secondly it is necessary to predict in these environments the behavior of dangerous chemical species (here particularly heavy metals) in the long term. This study focuses mainly on a detailed characterization of 4 soil samples sampled in vicinity of wild dump-BOULIMAT located 15 km west of the city of Bejaia-Algeria. The samples were characterised by atomic absorption spectrometry, X-ray diffraction, Fluorescence X and Infrared spectroscopy. The data showed high concentrations of metallic elements especially Zn (2,651.8 $mg.kg^{-1}$) and Ni (163.44 $mg.kg^{-1}$) in the soil samples. For their remediation, the stabilization/solidification (S/S) process with hydraulic binders appeared promising in reducing the polluting power of metal. This approach has considerably reduced the content of pollutants; 98 % removal was obtained for Ni and 99 % for Zn. The XRD analysis technique revealed the occurrence or absence of metallic elements in the crystallized phases.

Introduction

For a long time, waste and landfills have posed a serious problem leading to various environmental issues that industries have created, and developing several diseases including respiratory, dermatological or other. Human is the main driver of technological and scientific development through these innovations that make life simplier and easier, however, he is the main author of pollution generation at the scale industrial (mining, steel, etc.) or domestic (civil) such as household waste, hospital waste (Stuart *et al.* 1998; Sefouhi *et al.* 2010; Prasadini *et al.* 2014). Wastes (solid, liquid, gas) produced are released into the environment in the form of landfills, which are mostly uncontrolled, and in the presence of water, air and in contact with the receiving environment, becomes an active source of pollution developing complex and toxic elements with high geochemical mobility (Sefouhi *et al.* 2010), which are easy to transport and transfer (Prasadini *et al.* 2014), contaminating all the environment of proximity (air, soil, waters), thus influencing the life of the individual by the development of several diseases (cutaneous, pulmonary, neurological, etc.) causing an imbalance in the chain of life (Stuart *et al.* 1998; Sefouhi *et al.* 2010; Prasadini *et al.* 2014; Belebchouche *et al.* 2014).

A range of tests and experiments have been conducted in recent years on the analysis and characterization of waste, leaching and modeling

✉ *Corresponding author:* karimmoussaceb@yahoo.fr

of long-term waste behavior (Bozkurt *et al.* 2000). Accordingly, this work has two objectives. The first is characterization of the site hosting the wild discharge of the region of BOULIMAT-Bejaia, which opens with all the types of rejections, by determining the physico-chemical parameters (pH, conductivity, moisture), amount of material and particle sizes (granulometry) (Qiao *et al.* 2007; Chikhi *et al.* 2012), composition and chemical speciation (XRD, FX, FTIR, TCLP, AAS) (Windt *et al.* 2007) soils that define the nature and the intrinsic parameters of the discharges (Planel *et al.* 2004; Laforest *et al.* 2007), the second objective is to study of the evolution of the soil stability by the addition of hydraulic binders (Zampori *et al.* 2009; Drouiche *et al.* 2019).

The S/S method is an innovative method, which has been proven in the field by its treatment of more than 57 toxic elements (Gollmann *et al.* 2010; Du *et al.* 2010; Moussaceb *et al.* 2012; Moussaceb *et al.* 2013) by: (i) chemical stabilization of toxic element by adsorption and/or ion exchange which is the consequence of the formation of chemical bonds between the waste and the hydraulic binder (Fuessle *et al.* 2004; Moussaceb *et al.* 2012; EPA 2014), (ii) solidification by the transformation of waste into a solid monolith for the purpose of trapping contaminating species inside the cementitious matrices (Shi *et al.* 2004; Moussaceb *et al.* 2012; EPA 2014) thus reducing the mobility of toxic chemical species (EPA 2014) that focus primarily on the addition of a hydraulic binder (Portland cement) to contaminated soil (Moussaceb *et al.* 2012).

According to (Laurent *et al.* 2007) a study of S/S on samples of contaminated soil performed for 28 days to 1 year made the soil non-dangerous. Further (Rémillard 2012), reported that the decontamination of the soil contaminated with Cd, Cr, Cu, Pb, Zn (Shannon, Municipality, Canada) with S/S showed very good trapping results even after a long leaching period. Tests conducted by Soliditech. Inc. on a site contaminated by Pb and PCB in the region Morganville, New Jersey (USA) demonstrates a good application potential of the method (Bisson *et al.* 2012). Preliminary results of soil samples from the site examined in this work showed a high zinc and nickel content, thus presenting a site overload by these two elements.

The soil samples treated by the S/S process for a 28-day curing period, showed retention rates in Zn/Ni metals of up to 99 % in the cementitious matrices.

Experimental

For an eventual physico-chemical and mechanical analysis of our soil samples, an arsenal of standardized methods (FX, XRD, FTIR, AAS) as well as standardized tests (granulometry, humidity, electrical conductivity, pH, TCLP) were used to achieve our objectives, namely: (i) determination of the intrinsic properties of the contaminated soil samples, (ii) improvement of the trapping of heavy metals inside the cementitious matrices (Segolene 1992).

Sampling

Sampling was carried out at the BOULIMAT-Bejaia landfill site after shovelling and evacuation of the first two centimeters with a stainless shovel, four soil samples to a depth of up to 40 cm were carried out according to the method of Targeted Sampling according to ISO 1993 and EPA 1991. The sampling points are shown in Fig. 1 and their coordinates in Table 1 (Pellet *et al.* 1993; Liliane *et al.* 2007; Bisson *et al.* 2012).

Table 1. Location of soil sampling points with the decimal degree system (DDS).

Sample Index	Latitude (N) ° X	Longitude(E) ° Y
E (I)	36.789016	5.007027
E (II)	36.789283	5.007847
E (III)	36.789030	5.008666
E (IV)	36.788747	5.009202

Determination of selected physical parameters

The soil samples were treated according to ISO 11464, which consists of drying in the open air for 15 days before proceeding to physico-chemical analyzes (Pellet *et al.* 1993; Ministère du Développement Durable, de l'Environnement et des Parcs du QUEBEC 2010; Bisson *et al.* 2012).

Sieving granulometry determined the particle size distribution of soil by fractionation on the Shakers SV008 sieving machine according to AFNOR NF

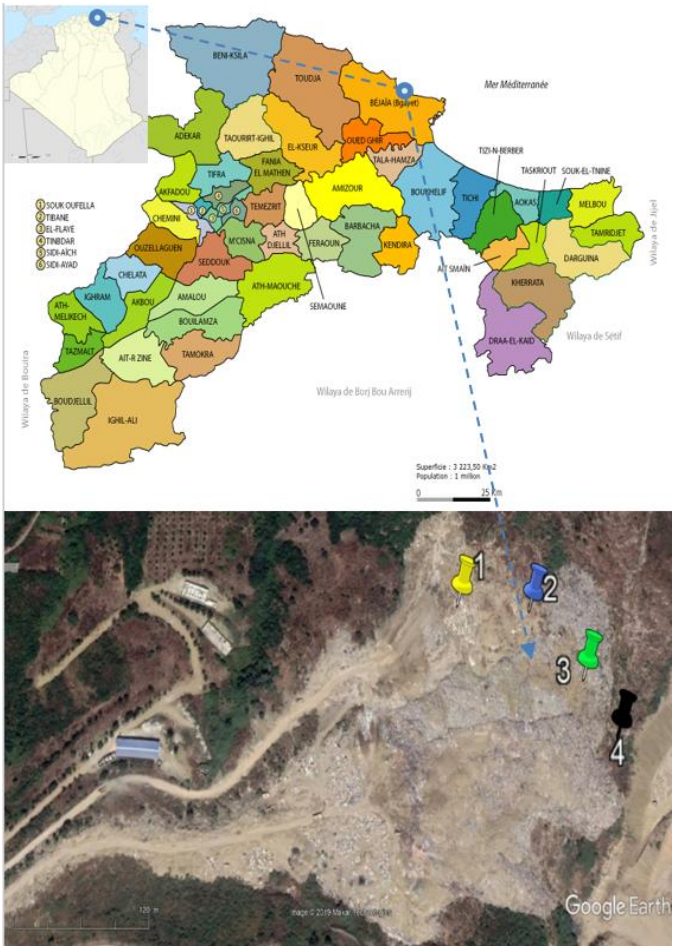

Fig. 1. Sampling points of the BOULIMAT-Bejaia landfill, the number 1-4 correspond to samplings sites of the samples EI-EIV (Table 1).

X31-101 (Violaine 2007; Bisson *et al.* 2012). Residual moisture measurement determined the dry mass lost of a soil sample dried at 103±3 °C whose mass is constant at 40 °C, according to AFNOR NF X31-102 (Segolene 1992; Marie *et al.* 2012). pH (H_2O) of soils was determined according to AFNOR X 31-103 recommends with the HANNA pH211 device (Segolene 1992; Liliane 2007; Kebir 2012). Electrical conductivity was determined by the dissolution of a soil sample in water according to the solid/liquid ratio, and which is measured with the apparatus HANNA EC215, according to AFNOR NF X 31-113 (Segolene 1992).

$$S/L = 1/5 \quad \ldots\ldots\ldots\ldots\ldots (1)$$

Mineralogical composition – X-ray diffraction (XRD)

X-ray diffraction consists in the identification of minerals by electron bombardment in the form of electromagnetic waves, where the atoms follow a specific arrangement according to the crystalline planes following to the BRAGG law.

$$n\lambda = 2d * Sin\Theta° \quad \ldots\ldots\ldots\ldots (2)$$

where n – diffraction order, λ – X-Ray wavelength, d – inter-reticular distance, Θ° – Bragg Angle. The indexation of peaks allows the identification of mineralogical phases present by referring to the American Society or Testing Materials (ASTM) sheets. The diffractograms of our soil samples were obtained on the device after treatment with Panalatical X'pert Hight Score (Ministère du Développement Durable, de l'Environnement et des Parcs du QUEBEC 2010; Marie *et al.* 2012; Eti 2012; Moussaceb *et al*. 2019).

Fourier Transform Infra-Red (FTIR) spectrometry

The FTIR is used to identify the functional groups existing within our soil samples following a vibrational transition interval between 4000 – 400 cm^{-1} (Mejbri *et al.* 1995; Mounia 2013) with the spectrometer SHIMADZU IRAffinity-1S, samples preparation is made in KBr pellet.

Chemical composition

The simple extraction procedures are methods that run in one step, and those using several methods. These concluded: (i) X-ray fluorescence, which gives the proportions of the major elements as an oxide by bombardment of the sample surface with X photons, performed using the SKYRAY 7000XRF experimental setup. (ii) atomic absorption spectrometry (Thermo Scientific ICE 3000) was used for the quantification of trace elements present in soil samples to be treated and those after acid leaching preparation (Toxicity Characterisation Leaching Procedure – TCLP) (Bisson *et al.* 2012; Drouiche *et al.* 2019).

Leaching tests

The TCLP-EPA 1311 test is a method used to evaluate the mobility of inorganic species in order to evaluate whether an industrial residue is considered as a dangerous leachable material or not.

It is carried out by dissolving a soil sample in a solution containing 2.572 g of sodium hydroxide and 5.7 mL of acetic acid with a solid/liquid ratio:

$$S/L = 1/20 \quad \ldots\ldots (3)$$

where the leachate recovered after filtration was analyzed for heavy metals by atomic absorption spectroscopy (AAS) (Lassin 2002; Liliane 2007; Moussaceb *et al*. 2019).

Soil samples processing

Once the soil samples have been characterized, an operation of treatment was carried out, and for this purpose mixtures of several variation were established by addition of contaminated soil (between 0 and 40 %) and cement. The cement used in this study is Portland cement CEM I from Ain El Kbira, Algeria. Table 2 shows the formulations made in accordance with standard NF P 98-230-3 (Bozkurt *et al.* 2000; Prasadini *et al*. 2014). The constituents were introduced into a mixer and mixed dry for 2 min. then they spread on a non-contaminating surface at the thickness of the largest grain and then the water is added by spraying and they are left for 28 days at a ambient temperature (20±3 °C) to undergo characterization tests, namely: XRD, FX, TCLP (Berger 2009). The realization of the mixtures soil/ cement is based on the report (Bouzeroura *et al*. 2018).

$$w/(c+s) = 0.5 \quad \ldots\ldots (4)$$

with: w – mixing water [mL], c – Portland cement [g], s – contaminated soil [g]. The quantities of cement are fixed at 450 g and those of the soil are varied from 0 to 40 %. The quantities used are given in Table 2.

Table 2. Mixtures formulations with quantity of cement (M_c), water (W) and soil (S).

M_c+S [g]	M_c [g]	W [mL]	S [g]	(s/c) ×100 [%]	w/(s+c)
495	450	247.5	45	10	0.5
540	450	270	90	20	0.5
585	450	292.5	135	30	0.5
630	450	315	180	40	0.5

Table 3. Granulometry parameters of soil samples (Jerome *et al*. 2012).

	Laws and Parameters	Unit	EI	EII	EIII	EIV
D5	Particles Diameter at 5 %	mm	0.09	0.13	0.10	0.07
D10	Particles Diameter at 10 %	mm	0.18	0.27	0.23	0.11
D16	Particles Diameter at 16 %	mm	0.33	0.45	0.39	0.18
D25	Particles Diameter at 25 %	mm	0.61	0.76	0.67	0.34
D30	Particles Diameter at 30 %	mm	0.91	0.98	0.87	0.48
D50	Particles Diameter at 50 %	mm	1.48	1.75	1.45	1.23
D60	Particles Diameter at 60 %	mm	1.88	1.97	1.79	1.62
D75	Particles Diameter at 75 %	mm	2.52	2.5	2.45	2.32
D84	Particles Diameter at 84 %	mm	2.98	3.02	2.93	2.84
D90	Particles Diameter at 90 %	mm	3.30	3.34	3.29	3.24
D95	Particles Diameter at 95 %	mm	3.65	3.66	3.63	3.57
Curvature coefficient	$C_c = D_{30}^2/D_{60} * D_{10}$	Cte	2.44	1.80	1.84	1.29
Uniformity coefficient	$C_u = D_{60}/D_{10}$	Cte	10.44	7.29	7.78	14.72
Sorting index (Trask)	$So = \sqrt{\frac{D_{75}}{D_{25}}}$	Cte	2.03	1.83	1.91	2.61
Asymmetric Trask coefficient	$Sk = \frac{D_{25} * D_{75}}{D_{50}^2}$	Cte	0.70	0.63	0.78	0.52
Inter-quartile	$\Delta = \sqrt{D_{84}/D_{16}}$	Cte	3.00	2.59	2.74	3.97
Angularity coefficient (Kurtosis)	$K = \frac{(D_{75}-D_{25})}{2*(D_{90}-D_{10})}$	Cte	0.30	0.29	0.29	0.31
Porosity	$P = 0.13 + \frac{0.21}{(D_{50}+0.002)^{0.21}}$	mm^{-1}	0.32	1.75	2.11	2.54
Dispersion index (FOLK/WARD)	$D = \frac{(D_{84}-D_{16})}{4} + \frac{(D_{95}+D_5)}{6.6}$	mm	1.20	1.17	1.17	1.19
Asymmetric index of Krumbein	$Sk_i = \frac{(D_{75}+D_{25})-(2*D_{50})}{2}$	mm	0.085	0.085	0.11	0.10

Results and Discussion

Characterisation of sampled, non-treated soil

Granulometry distribution was rather similar for tested soil samples (for EI shown in Fig. 2A) from values of individual parameters (Table 3) it can be seen that the values of the coefficients recorded are as follows: curvature coefficient ranged between 1.29 – 2.44, uniformity coefficient between 7.29 – 14.72, sorting index (Trask) between 1.83 – 2.61, asymmetric Trask coefficient between 0.52 – 0.78, inter-quartile between 2.59 – 3.97, angularity coefficient (Kurtosis) between 0.29 – 0.31, porosity in range of 0.31 – 0.33, dispersion index (Folk/Ward) between 1.16 – 1.20, asymmetric index of Krumbein in range of 0.085 – 0.11.

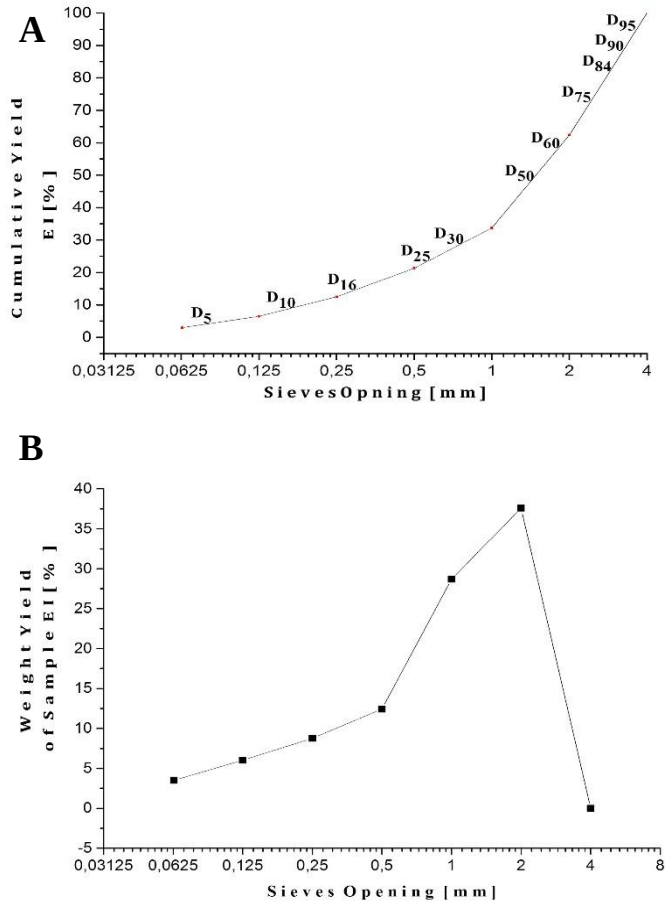

Fig. 2. Characterisation of non-treated soil samples. Granulometry distribution of soil sample EI and the grain diameters at percentage between 5 % to 95 % corresponding to D_5 to D_{95} (**A**). Weight distribution of the same soil sample according to sieves series in range 0.063 – 4 mm, depending on the AFNOR NF X31-101 standard (**B**) corresponding data are given in Table 3.

These data point on a varied grain size, a spread and poorly graded distribution, and a ranking of the grain size on the coarse fraction side with a random arrangement of poorly sorted spheres. (Blott and Pye 2001; Jerome *et al*. 2012). Thus, our samples represent a spreading and well graded particle size.

The results in Fig. 2B show the weight distribution of sample EI. Highly similar pattern was observed for the weight distribution of EII-EIV samples (data not shown). It is concluded that our soil samples have the same weight proportions with a high mass presence at mean diameters (2 and 1.5 mm). These represent respectively the intervals 2 – 1 mm and d > 2mm, and which vary between 32.34 % – 39.57 % and 25.4 % – 32.25 %, respectively. According to the standard NF P18-560 and according to the classifications of Strakhov and Wentworth (Jerome *et al*. 2012), it is concluded that our soil is coarse sand-type.

The main properties of soil samples are shown in Table 4. The data show that the moisture content varies between 1.11 % and 3.10 %. These values are strongly linked to actual climatological factors during the moment of sampling just after the summer period of 2016/2017, as well as the presence of waste that makes the soil hydrophobic to water. According to Souhila (2005) the loss of mass in the soil does not only refer to water but also to the evaporation of volatile organic matter likely to intervene at 60 °C. The pH of soil samples varies between 8.05 and 8.25 (Table 4), suggesting that the soil is an alkaline soil (Marie 2009), favoured by the dominant geological formation of the study site which is calcareous-sedimentary formation. According to Souhila (2005) basic pH values have been found in the geological state of the studied soil and which is alkaline. Furthermore, Kebir (2012) reports that the basic pH of soil samples of the landfill refers to biological activity in field.

Table 4. Physical parameters of soil samples according to AFNOR NF X31 standards.

Sample	Moisture [%]	pH (H_2O)	Conductivity [mS.Cm^{-1}]
E I	3.05	8.20	689
E II	2.47	8.05	1173
E III	3.10	8.10	958
E IV	1.11	8.25	519

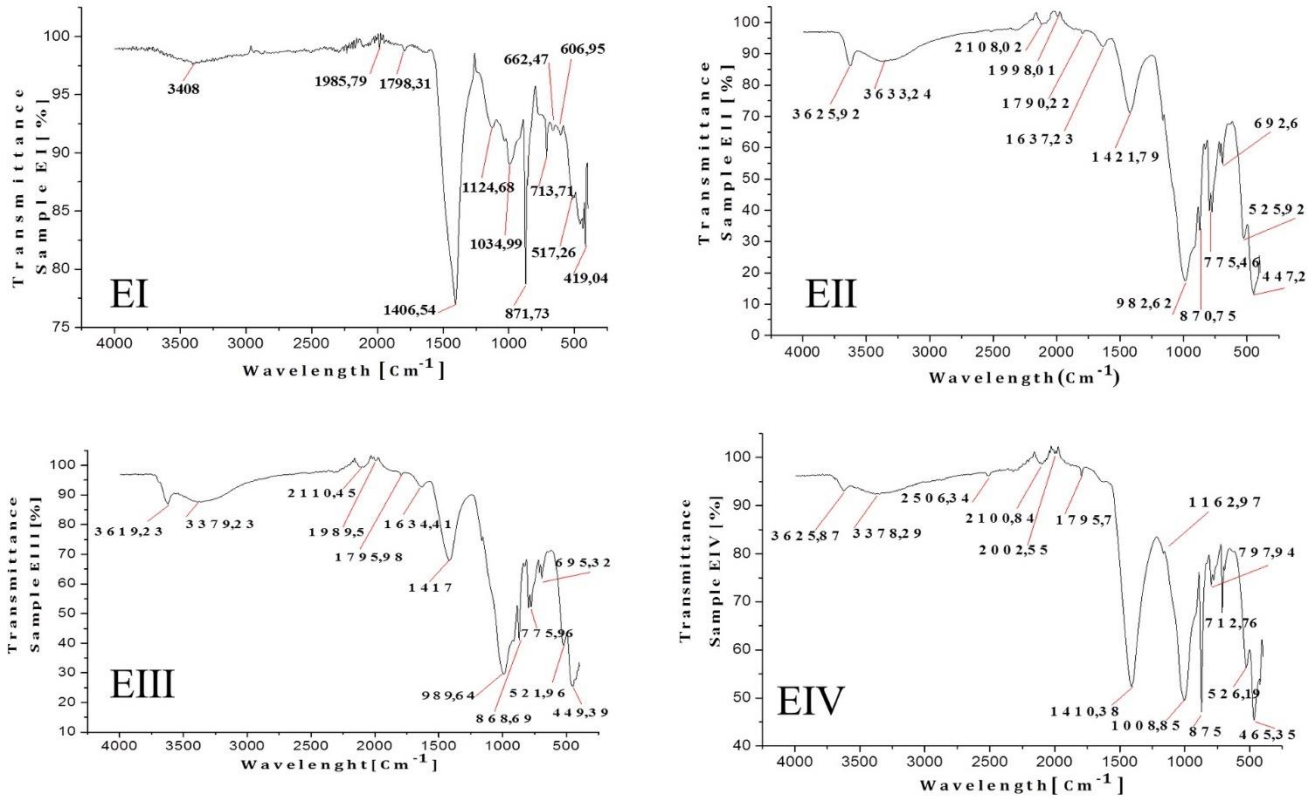

Fig. 3. Infrared spectrum of soil samples from localities EI-EIV (Fig. 1) before treatment.

The values of conductivities range from 519 to 1,173 mS.cm^{-1}, which is classified as slightly saline soil according to DURAN scale (Marie 2009). These values indicate a strong interaction between the salts present in the soil and the mineral character of the study site.

Fourier transform infrared spectroscopy (FTIR) was applied to identify functional groups. The analysed soil samples have a high siliceous rock content, which has a vibrational domain at 2,100 cm^{-1} and 1986 cm^{-1} and then at 1,124 cm^{-1} and 1162 cm^{-1}. For calcareous rock, there are strong transition at 2506 cm^{-1}, 1,790 cm^{-1} and 1,400 cm^{-1}, whereas the vibrational plugs of the intermolecular water appear at 3,408 cm^{-1}, 3,364 cm^{-1}, 3,396 cm^{-1} and 3,378 cm^{-1} for samples EI, EII, EIII and EIV, respectively. The latter reappear at 1,637 cm^{-1} and 1,634 cm^{-1} for EII and EIII, respectively. Similar results were found from an FTIR characterization study on soil samples from southern Brazil (Dick 2003). Table 5 summarizes the overall results for each soil samples. The infrared spectrum from soil samples is presented in Fig. 3 and corresponding functional groups are characterised in Table 5.

The results of X-ray fluorescence showed that soil samples EI, EII and EIII have high proportions of SiO_2, ranging from 45.80 % to 50.37 %, and Al_2O_3 ranging from 13.77 % to 15.09 % (Table 6). A low CaO content of 11.67 % to 18.39 % was recorded as well. On the other hand, the soil sample IV has a high proportion of CaO, which is of the order of 48.39 % and low levels of SiO_2 and Al_2O_3 (19.06 % and 7.27 %, respectively). The presence of metal elements in small proportions in the form of traces has been observed. These results can be explained by the fact that the soil samples EI, EII and EIII were taken in places with a high presence of silica and alumina, resulting from the rejections of the discharge in question, which consist of glasses and aluminum, and their provenance from the mother rock of the region which is rich in silicates and aluminates. On the other hand, the results obtained in the soil sample EIV are confirmed by the fact that the sampling was carried out on the eastern periphery of the landfill and close to a limestone bed (aggregate quarry).

The metallic trace elements found in these soil samples returned to the nature of the waste

Table 5. Infrared spectroscopy of the functional groups from soils samples using SHIMADZU IRAffinity-1S (Foil *et al.* 1952; Maglione *et al.* 1975).

Soil Sample Wavelength [Cm^{-1}]				Identification Band
EI	**EII**	**EIII**	**EIV**	
ND	3626	3623	3626	Vibration Si-O-H of Clay
3408	3363	3396	3378	Vibration OH of H_2O
ND	ND	ND	2506	Calcite
ND	2108	2111	2101	Vibration Si-O of Quartz
1986	1998	1990	2003	Vibration Si-O of Quartz
1798	1790	1796	1796	Calcite
ND	1637	1634	ND	Vibration OH of H_2O
1407	1422	1406	1410	Calcite
1125	ND	ND	1163	Si-O of Quartz
1035	983	1002	1009	Vibration of Si-O of Alumino-Silicate
872	871	874	875	Vibration of CO_3 of $CaCO_3$
ND	776	776	798	Vibration of CO_3 of $CaCO_3$
714	ND	710	713	Vibration of CO_3 of $CaCO_3$
ND	693	695	ND	Calcite/Quartz
663	ND	ND	ND	ND
607	ND	ND	ND	ND
517	526	522	526	Vibration of SI-O-Al
419	447	449	465	Vibration of Si-O-Si

discharged into the landfill (household, hospital, urban and industrial waste, etc.). According to Antonine (2012) the high abundance of $CaCO_3$ content refers to the presence of carbonates in rocks of study site and for metallic minerals in the form of hydroxide or sulphide. The chemical compositions of analysed soil samples are shown in Table 6.

The leachates obtained by dissolving (TCLP test) were subjected to a chemical analysis, by AAS, to determine the contents of the metallic elements. It is found that the contents of the soil samples (Table 6) perfectly meet the AFNOR NF U44-041 (1985) (Segolene 1992) standard except for [Ni] > 50 $mg.kg^{-1}$ in the soil sample EI and [Zn] > 300 $mg.kg^{-1}$ in the soil sample EIII. The results shown in Table 6 can be justified by acid rain, which frequently affects the region, thus promoting the migration of heavy metals through leachates that percolate from the landfill to the surrounding soil. According to Kebir (2012) the persistence of these metallic elements concentrations refers to the origin of the waste as well as to the industrial effluents discharged into the landfill.

According to the XRD results, the soil has a similarity in initial mineralogical composition, which is a clay soil consisting mainly of quartz and calcite, with heterogeneity in the secondary phases that show contamination with heavy metals. Examples include Dwornikite and Retgersite for EI and Wurtzite, Hopeite and Hetaerolite for EIII. The diffractograms of soil samples EI and EIII are shown in Fig. 4, while the corresponding mineralogical phases are summarized in Table 7.

Table 6. Chemical composition of the analysed soil samples from localities E-EIV.

	Soil sample			
	EI	**EII**	**EIII**	**EIV**
Compound content [%] [a]				
SiO_2	**50.37**	**47.07**	**45.80**	**19.6**
Al_2O_3	**15.9**	**13.77**	**14.9**	**7.27**
Fe_2O_3	4.74	5.2	5.14	4.17
CaO	**11.67**	**16.20**	**18.39**	**48.39**
MgO	<0.05	ND	ND	0.79
Na_2O	<0.05	<0.05	<0.05	<0.05
K_2O	2.7	2.2	2.4	1.7
TiO_2	0.48	0.46	0.48	0.23
MnO	0.09	0.20	0.13	0.19
P_2O_5	0.28	0.42	0.35	0.76
SO_3	0.09	0.15	0.05	0.021
NiO	**0.0028**	**0.0035**	**0.0026**	**<0.005**
ZnO	**0.0088**	**0.0071**	**0.0056**	**0.019**
PbO	0.0031	0.0028	0.0057	0.0123
Metal content [$mg.kg^{-1}$] [b]				
Zn	9.388	4.194	**2651.8**	20.78
Ni	**163.44**	38.3	0.22	<Ld
Pb	0.4	<Ld	3.4	2

[a] Data obtained by X-ray fluorescence.
[b] According to AFNOR NF U44-041 standard, after TCLP leaching test.

Table 7. Mineralogical Composition of EI Sample using X'pert High Score.

Mineral phases	Chemical composition	References pattern
Soil sample EI		
Quartz	SiO_2	01-078-1252
Calcite	$CaCO_3$	01-083-1762
Urea	$CO(NH_2)_2$	01-086-2276
Muscovite	$KAl_3Si_3O_{10}(OH)_2$	01-075-0948
Despujolsite	$Ca_3Mn(SO_4)_2(OH)_6(H_2O)_3$	01-072-0388
Tridymite	SiO_2	01-075-1323
Dwornikite	$(Ni, Fe)SO_4.H_2O$	00-035-0558
Argentopyrite	$AgFe_2S_3$	00-038-0459
Domeykite	Cu_3As	00-044-1475
Manganotapiolite	$(Mn, Fe)Ta_2$	00-049-1870
Retgersite	$NiSO_4(H_2O)_6$	01-075-0937
Kyanite	Al_2SiO_5	01-076-0170
Hatrurite	Ca_3SiO_5	01-086-0402
Soil sample EIII		
Hetaerolite	Mn_2O_4Zn	00-024-1133
Rostite	$Al(SO_4)(OH).5H_2O$	00-041-1382
Quartz	SiO_2	01-078-1252
Calcite	$CaCO_3$	01-083-0578
Hopeite	$Zn_3(PO_4)_2.4H_2O$	00-001-0975
Halloysite	$Al_2Si_2O_5(OH)_4$	00-003-0184
Sarcopside	$Fe_3(PO_4)_2$	00-039-0341
Anthophyllite	$Mg_7(Si_8O_{22}(OH)_2)$	01-075-0909
Collinsite	$Ca_2Mg(PO_4)_2.2H_2O$	00-026-1063
Clinzoisite	$Ca_2Al_3(SiO_4)\ (Si_2O_7)(O, OH)_2$	00-021-0128
Chalcocite	Cu_2S	00-023-0961
Wurtzite	ZnS	01-072-0162
Reinhardraunsite	$Ca_5(SiO_4)_2(OH)_2$	00-029-0380
Linthian Saponite	$Na_{0,2}(Mg,Li)_3Si_4O_{10}(OH)_2.4H_2O$	00-025-1385
Quartz	SiO_2	01-078-1252
Calcite	$CaCO_3$	01-083-1762
Urea	$CO(NH_2)_2$	01-086-2276
Muscovite	$KAl_3Si_3O_{10}(OH)_2$	01-075-0948
Despujolsite	$Ca_3Mn(SO_4)_2(OH)_6(H_2O)_3$	01-072-0388
Tridymite	SiO_2	01-075-1323
Dwornikite	$(Ni, Fe)SO_4.H_2O$	00-035-0558
Argentopyrite	$AgFe_2S_3$	00-038-0459
Domeykite	Cu_3As	00-044-1475
Manganotapiolite	$(Mn, Fe)Ta_2$	00-049-1870
Retgersite	$NiSO_4(H_2O)_6$	01-075-0937
Kyanite	Al_2SiO_5	01-076-0170
Hatrurite	Ca_3SiO_5	01-086-0402

It is concluded that physico-chemical characterization study of the project site samples, which all the results obtained; converge towards the same conclusion suggest contamination of the site by zinc and nickel, posing a great danger to the environment, fauna and flora as well as to human health.

Characterization of S/S soil samples

Decontamination of the contaminated sites is imperative, therefore a soil process has been proposed, namely remediation by S/S process with hydraulic binders. After such treatment, FTIR analysis revealed the disappearance of several vibrational bungs and the appearance of others such as ettringite at 3,400 cm^{-1} and C-S-H at 1,400 cm^{-1} and 1,000 cm^{-1} (Fig. 5). Further, the bung of calcite was detected. Similar results were found in a study reported by Catherine (2003). The functional groups corresponding to data in Fig. 5 are given in Table 8.

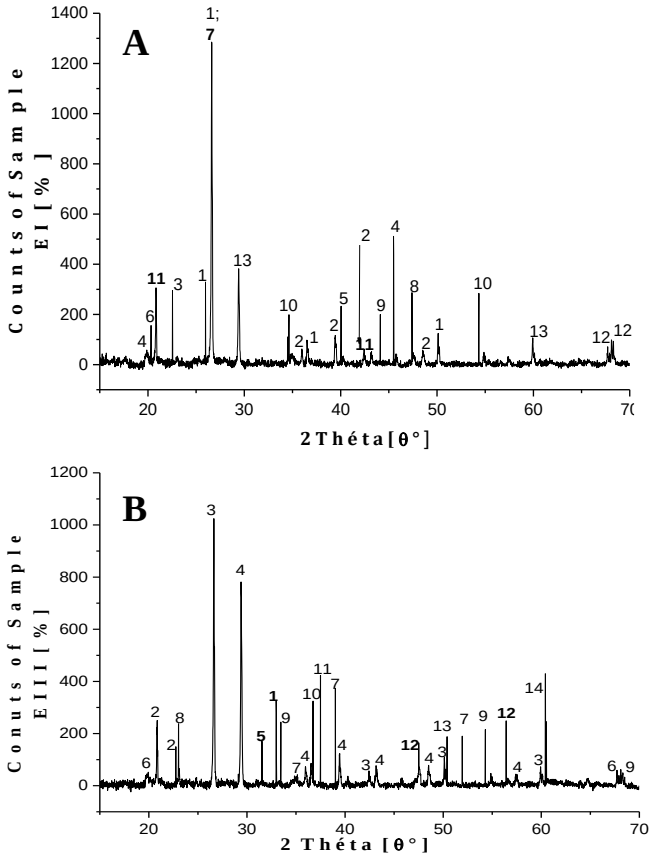

Fig. 4. X-ray diffraction of non-treated soil samples EI (**A**) and EIII (**B**) after treatment with Panalatical X'pert Hight Score.

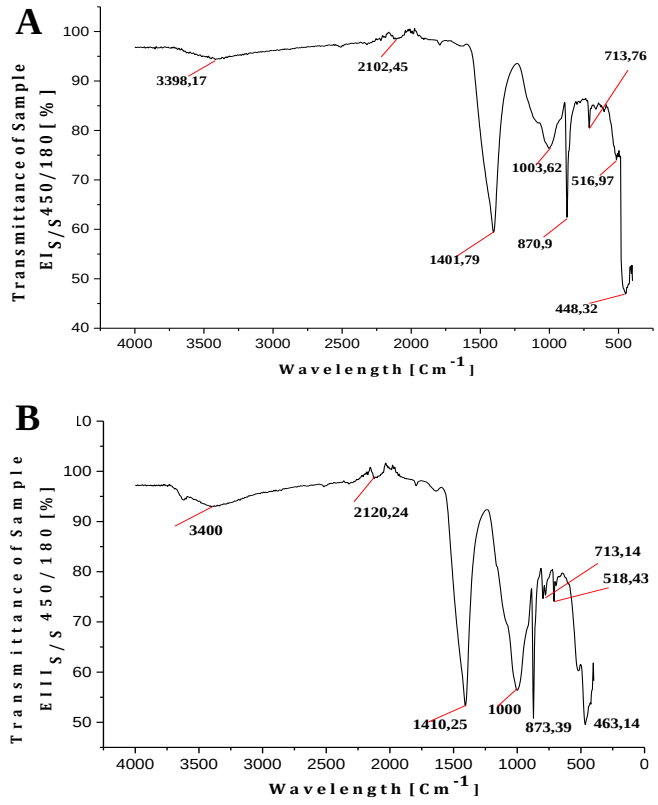

Fig. 5. Infrared spectra of the stabilized / solidified soil sample $EI_{S/S}$450/180 (**A**) and $EIII_{S/S}$450/180 (**B**).

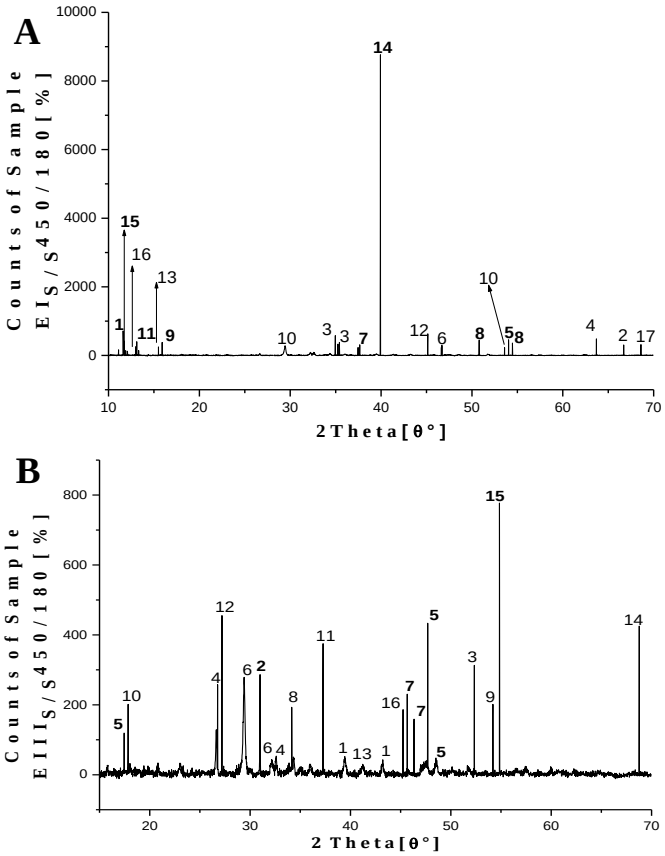

Fig. 6. X-ray diffraction of soil samples $EI_{S/S}$ (450/180) (**A**) and $EIII_{S/S}$ (450/180) (**B**) after treatment with Panalatical X'pert Hight Score**.**

Table 8. Infrared spectroscopy of the functional groups from Stabilized/Solidified samples soils using SHIMADZU IRAffinity-1S.

Wavelengths for each Samples (Cm^{-1})		
$EI_{S/S}$	$EIII_{S/S}$	**Identification Band**
3398	3400	Hydrated Ettringite
2103	2120	Vibration OH (H_2O)
1402	1410	C.S.H
1004	1000	C.S.H
871	873	Ettringite
714	713	Vibration of CO_3 ($CaCO_3$)
517	518	Gibbsite
448	463	Gibbsite/Silicate

The X-ray fluorescence results obtained on the EI and EIII samples of the S/S soil are recorded in Fig. 6 and Table 9. The results obtained show that CaO content in soil samples EI and EIII decreased due to remediation process from 11.67 % and 18.39 % (before S/S) to 46.08 % and 55.84 % (respectively), due to the accumulation of CaO proportions present in the soil and the cement after the hydration phenomenon On the other hand, content of both SiO_2 and Al_2O_3 decreased after S/S;

Table 9. Chemical composition from soil sample $EI_{S/S}$450/180 in oxidation form by the X-ray fluorescence.

Sample ($E_{S/S}$)	$EI_{S/S}$					$EIII_{S/S}$				
	450/0	**450/45**	**450/90**	**450/135**	**450/180**	**450/0**	**450/45**	**450/90**	**450/135**	**450/180**
***Cement/Soil*[a]**										
SiO_2	**14.62**	**12.82**	**17.47**	**17.83**	**16,82**	**14.62**	**15.26**	**16.55**	**19.41**	**21.23**
Al_2O_3	**2.4**	**3.9**	**2.62**	**2.76**	**2.5**	**2.4**	**2.6**	**2.5**	**2.9**	**3.49**
Fe_2O_3	2.31	3.9	2.86	2.94	2.71	2.31	2.58	2.74	2.97	3.26
CaO	**53.00**	**46.08**	**48.13**	**48.26**	**51.35**	**53.00**	**51.86**	**49.49**	**48.86**	**46.06**
MgO	1.36	1.55	1.5	1.65	1.7	1.36	1.25	1.38	1.58	<LD
K_2O	0.52	0.67	0.58	0.59	0.58	0.52	0.55	0.56	0.67	0.77
TiO_2	0.20	0.37	0.27	0.31	0.25	0.20	0.23	0.25	0.3	0.34
MnO	0.04	0.04	0.048	0.044	0.041	0.04	0.05	0.05	0.05	0.06
P_2O_5	1.5	0.98	0.95	1.6	1.4	1.5	1.3	0.93	0.98	0.82
SO_3	<LD	0.12	0.014	0.007	<LD	<LD	<LD	<LD	<LD	0.17
NiO	<LD	<LD	<LD	<LD	<LD	<LD	<LD	<LD	<LD	<LD
ZnO	<LD	<LD	<LD	<LD	<LD	<LD	<LD	<LD	<LD	<LD
PbO	<LD	<LD	<LD	<LD	<LD	<LD	<LD	<LD	<LD	<LD
***Metal content*[b]**										
Ni [mg.kg^{-1}]	nd	0.17	0.32	0.42	1.69	nd	nd	nd	nd	nd
Retentions rate [%]	nd	97.68	97.82	98.09	94.25	nd	nd	nd	nd	nd
Zn [mg.kg^{-1}]	nd	nd	nd	nd	nd	nd	0.21	9.1	23.73	30.70
Retentions rate [%]	nd	nd	nd	nd	nd	nd	99.82	96.22	93.37	93.56

[a] Data obtained by X-ray fluorescence.
[b] According to AFNOR NF U44-041 standard, after TCLP leaching.

the SiO_2 content dropped from 50.37 % and 45.80 % of the two samples to 12.82 % and 15.26 % after S/S, respectively. This decrease results from incorporation of SiO_2 from Quartz. As for Al_2O_3 the values of 15.09 % and 14.09 % of non-treated EI and EIII soil samples decrease to 3.09 % and 2.06 % after S/S, respectively. This decrease is due to growth of hydration phases of cement and more specifically C.S.H and ettringite for Al_2O_3.

The presence of SO_3 in our S/S materials refers to the formation of the cement phase (ettringite) as well as the presence of sulphur in the soil and cement. The variation of the values of Si, Al, S and Ca refer to the hydration reaction between the materials of soil and those of hydraulic binder; they are mobilised to form hydrates of cements after S/S (Saussaye *et al.* 2016). On the other hand, the absence of the metallic oxides in the samples before S/S can be explained by the mechanism of substitution of elements with those of cement and which made it possible to trap chemically and physically the metallic elements inside cement matrix. S/S of soil samples resulted in strong retention of the contents of Ni and Zn; their content increased to 98.09 % for (Ni) and 99.82 % for (Zn) in the soil samples EIII and EI, respectively (Table 9).

X-Ray diffraction results obtained on S/S treated sample EI (450/180) and EIII (450/180) are given in Fig. 6. The soil sample EI exerted disappearance of certain mineralogical phases such as retgersite ($NiSO_4$ $(H_2O)_6$), but the appearance of other mineralogical phases such as sodium nickel sulfite hydroxide hydrate ($NaNi$ $(SO_3)_2$ OH H_2O). For soil sample EIII the disappearance of certain mineralogical phases such as hopeite (Zn_3 $(PO_4)_2$ $4H_2O$) and the appearance of other phases, such as descloizite (Pb (Zn, Cu) VO_4 (OH)) was observed in (Table 10).

Compared with the work of Berger (2009) on substitutions of metallic trace elements with the phases of cement (natural or synthetic, total or partial) we found that for the two phases found after S/S, there is a probability of substitution of (Ni) from sodium nickel sulfite hydroxide hydrate with (Al) of ettringite for sample EI, and (Pb, Zn) from descloizite with (Ca) of ettringite for Sample EIII (Table 11).

Conclusion

This study analyzed the influence of the addition of hydraulic binder to the contaminated soil as well as of the proportional addition from cement trapping of heavy metals in cementitious matrices. Our results showed that granulometric characteristic of soil

Table 10. Mineralogical composition of soil samples $EI_{S/S}$ (450/180) and $EIII_{S/S}$ (450/180) using X'pert High Score.

Mineral phase	Chemical composition	Reference pattern
Soil sample EI		
Sophiite	$Zn_2(SeO_3)Cl_2$	00-045-1463
Galaxite	$MnAl_2O_4$	00-001-1302
Fayalite	Fe_2SiO_4	01-071-1669
Ferrocarpholite	$(Fe_{0,76}Mg_{0,24})_2Al_4(Si_4O_{12})(OH)_8$	01-081-1503
Nickelbischofite	$NiCl_2.6H_2O$	00-025-1044
Ettringite	$Ca_6Al_2(SO_4)_3(OH)_{12}.25H_2O$	00-009-0414
Ammonium nickel chromium oxide hydrate	$(NH_4)_2Ni(CrO_4)_2.6H_2O$	00-021-0705
Nickelboussingaultite	$(NH_4)_2Ni(SO_4)_2.6H_2O$	00-031-0062
Nickel sulfite hydrate	$NiSO_3.2H_2O$	00-034-0315
Potassium nickel selenate hydrate	$K_2Ni(SeO_4)_2.6H_2O$	00-035-0774
Sodium nickel sulfite hydroxide hydrate	$NaNi_2OH(SO_3)_2.H_2O$	00-037-0016
Fersilicite	FeSi	00-038-1397
Nickel trans-[dichlorobis(2-oxopropyl-diphenylphosphine)]	$C_{30}H_{30}Cl_2NiO_2P_2$	00-040-1756
Brucite	$Mg(OH)_2$	01-082-2455
Clinohedrite	$CaZn(SiO_4)(H_2O)$	01-083-2269
Bementite	$Mn_{6,927}(Si_6O_{15})(OH)_8$	01-082-1236
Cummingtonite	$Mg_7Si_8O_{22}(OH)_2$	01-072-0114
Soil sample EIII		
Calcite	$CaCO_3$	01-083-0578
Tachyhydrite	$CaMg_2Cl_6.12H_2O$	00-034-0788
Burbankite	$(Na_2Ca)(Sr_2Ca)(CO_3)_5$	00-026-1374
Anilite	Cu_7S_4	00-024-0058
Descloizite	$Pb(Zn, Cu)VO_4(OH)$	00-041-1369
Reinhardbraunsite	$Ca_5(SiO_4)_2((OH)F)$	01-075-1709
Tobermorite	$(CaO)_x SiO_2 zH_2O$	00-006-0005
Brushite	$CaPO_3(OH).2H_2O$	00-009-0077
Zinc malonate dihydrate	$C_3H_2O_4Zn.2H_2O$	00-024-1990
Zinc selenate hydrate	$ZnSeO_4.H_2O$	00-026-0004
Pyrophyllite	$Al_2Si_4O_{10}(OH)_2$	01-074-1037
Quartz	SiO_2	01-083-2473
Ettringite	$Ca_6Al_2(SO_4)_3(OH)_{12}\cdot 26H_2O$	00-041-1451
Palmierite	$K_2Pb(SO_4)_2$	00-020-0902
Calcium zinc aluminium oxide	$Ca_3Al_4ZnO_{10}$	00-049-0280
Muscovite	$KAl_3Si_3O_{10}(OH)_2$	01-071-1049

Table 11. Mineralogical composition from the probability of substitution phases in selected soil samples.

Phase type	Chemical formula
Soil Sample EI $_{S/S}$ (450/180)	
Sodium nickel sulfite hydroxyde hydrate	$(Na\ Ni_2\ OH\ (SO_3)_2\ H_2O)$
Clinohedrite	$(CaZn)(SiO_4)(H_2O)$
Soil Sample EIII$_{S/S}$ (450/180)	
Descloizite	$(Pb\ (Zn, Cu)\ VO_4\ (OH))$
Calcium zinc aluminium oxide	$(Ca_3\ Al_4\ Zn\ O_{10})$

samples increased because the mineral composition of the limestone rocks dominates on the site, alkaline pH which defines the nature of the sedimentary rocks, and causes very high soil conductivities. We identified the profiles of present major elements as well as metallic elements in the mineralogical structure of soil samples. The high concentration of Ni and Zn detected in the soil surrounding the landfill probably results from leaching with acid rain that caused a migration of trace metallic elements from waste to soil.

The analyses and characterizations of our S/S samples revealed new functional groups belonging to cement phases such as ettringite and C.S.H. Further, X-ray Fluorescence results suggest that the metallic trace elements disappear from soils

because they are likely trapped inside the cementitious matrices. Elevated proportion of CaO and decreased contents of SiO_2 and Al_2O_3 in the soil samples might results from cement interaction with the soil during its hydration. AAS confirmed Ni and Zn retention rates of up to 98 %. X-ray Diffraction analyses revealed disappearance of certain mineralogical phases with metallic trace elements after the treatment. On the other hand, hydrated cement phases were identified, such as ettringite, portlandite and C.S.H in the form of tobermorite with presence of metallic trace elements. Substitution occurred between the metallic trace elements and the elements of the hydrated cement. It is concluded that the S/S process using hydraulic binders represents a promising method in the treatment of contaminated soils.

Conflict of Interest

The authors declare that they have no conflict of interest.

References

Antonine P (2012) Caractérisation multi-échelles des phases porteuses des polluants métalliques Zn et Pb dans un sédiment mis en dépôt De l'analyse de terrain au rayonnement synchrotron. University of Orléans, p. 31-33.

Belebchouche C, Moussaceb K, Tahakourt A, Ait-Mokhtar A (2014) Parameters controlling the release of hazardous waste (Ni^{2+}, $Pb^{2+}$and Cr^{3+}) Solidified/Stabilized by Cement-CEM I. Mater. Struct. 48: 2323-2338.

Berger S (2009) Etude des potentialités des ciments sulfo-alumineux bélitiques pour le conditionnement du zinc De l'hydratation à la durabilité. Université des Sciences et Technologie de Lille, Lille I., p. 24-29.

Bisson DL, Jackson DR, Williams KR, Grube WE (2012) Static leaching of solidified/stabilized hazardous waste from the soliditech process. J. Air Waste Manage. Assoc. 41: 1348-1354.

Blott SJ, Pye K (2001) Gradistat: A grain size distribution and statistics package for the analysis of unconsolidated sediment. Earth Surf. Process. Landf. 26: 1237-1248.

Bouzeroura M, Mouassaceb K (2018) Effectiveness of adding metallic fibers on the stabilization/solidification of the hydroxides by hydraulic binder. J. Solid Waste Technol. Manag. 44 : 193-205.

Bozkurt S, Moreno L, Neretnieks I (2000) Long term processes in waste deposits. Sci Total Environ. 250: 101-121.

Catherine FM (2003) Etude de matériaux a base de liant hydraulique contenant des polluants organiques modèles : Propriété structurales et de transfert. Institut National des Sciences Appliqués de Lyon, p. 98-102.

Chikhi M, Balaska F, Boudraa S, Boutibiba H (2012) Experimental study of stabilization of sludge containing toxic metal by hydraulic binders. Energy Proceed. 19: 259-268.

Dick DP, Santos JHZ, Ferranti EM (2003) Chemical characterization and infrared spectroscopy of soil organic matter from two southern brazilian soils. Revista Brasileira de Ciência do Solo 27: 29-39.

Drouiche CM, Moussaceb K, Emmanuel J, Bollinger JC (2019) Stabilization/solidification by hydraulic binders of metal elements from landfill leachate. Nova Biotechnol. Chim. 18: 72-83.

Du YJ, Liu SY, Liu ZB, Chen L, Zhang F, Jin F (2010) An overview of stabilization/solidification technique for heavy metals contaminated coils. *In* Chen Y, Zhan L, Tang X (eds) Advances in Environmental Geotechnics. Springer, Berlin, Heidelberg, p. 760-766.

Eti T (2012) Contamination de sols par des eléments traces métalliques en zone méditerranéenne côtière: etudes de leur mobilité et du transfert a la phytocénose. University Aix-Marseille, 108 p.

Foil AM, Charles HW (1952) Infrared and characteristic frequencies of inorganic ions. J. Anal. Chem. 24: 1253-1294.

Fuessle RW, Taylor MA (2004) Stabilization of arsenite wastes with prior oxidation. J. Environ. Eng. 130: 1063-1066.

Gollmann M, Da Silva M, Masuero AB, Dos Santos J (2010) Stabilization and solidification of Pb in cement matrices. J. Hazard. Mater. 179: 507-514.

Jerome F, Raphael P, Chantal BC, Monique LV (2012) Analyses granulométriques: Principes et methods practical school of high studies. National Center of Scientific Research (France) 15: 36-51.

Kebir T (2012) Étude de contamination, d'accumulation et de mobilité de quelques métaux lourds dans des légumes, des fruits et des sols agricoles situent près d'une décharge industrielle de l'usine alzinc de la ville de ghazaouet. University of Abou-Bekr Belkaid Telemcen, ALGERIA, 47, p. 100-127.

Laforest G, Duchesne J (2007) Investigation of stabilization/solidification of electric arc furnace dust: Dynamic leaching of, monolithic specimens. Cement Concrete Res. 37: 1639-1646.

Lassin A, Bodenan F, Piantone P, Blanc P (2002) Essais de comportement des déchets à la lixiviation et modélisation des processus <<Hydro-Physico-Chimiques>> associés. Etude Bibliographique. Rapport BRGM/RP-51518-FR, p. 17-20.

Laurent C (2007) Solidification/stabilisation des déchets dangereux- procédés à base de liants minéraux. Agence de l'environnement et de la maitrise de l'energie, ADEME - France, 6 p.

Liliane J (2007) Mobilisation du chrome et du nickel a partir de sols contaminés, en présence de complexant : transfer et accumulation de ces métaux chez datura innoxia. University of Limoges, France, p. 47-52.

Maglione G, Carn M (1975) Spectres infrarouges des matériaux salins et des silicates néoformés dans le bassin tchadien. Cahiers ORSTOM, ser. Géologie 7: 3-9.

Marie L (2012) Caractérisation physico-chimique d'un sédiment marin traité aux liants hydrauliques – évaluation de la mobilité potentielle des polluants inorganiques. National Institut of Applied Sciences of Lyon, France, p. 100-121.

Marie M (2009) Accélération de ciment au laitier par du ciment sulfo-alumineux. National Institut of Applied Sciences of Lyon, France, p. 98-99.

Mejbri R, Matejka G, Lafrance P, Mazet M (1995) Fractionnement et caractérisation de la matière organique des lixiviats de décharge d'ordures ménagères. Revue des Sciences de l'Eau 8: 217-236.

Ministére du Développement Durable, de l'Environnement et des Parcs du QUEBEC Guide D'échantillonnage A Des Fins D'analyses Environnementales : Cahier 5-Echantillonnage des Sols. (2010) QUEBEC. Centre d'Exprtise en Analyse Environnementale du QUEBEC, p. 41-44.

Mounia C (2013) Analyse et spéciation des métaux dans un oued en zone minière cas de l'oued essouk. University de Constantine 1, ALGERIA, 49 p.

Moussaceb K, Ait-Mokhtar A, Merabet D (2012) Influence of leaching conditions on the release kinetics of lead, chromium and nickel from solidified/stabilized cementitious materials. Environ. Technol. 33: 2681-2690.

Moussaceb K, Belebchouche C, Ait-Mokhtar A, Merabet D (2013) Evaluation of the impact of Ni, Cr and Pb contained in effluents of an industrial unit by the process of stabilization/solidification using hydraulic binders. Int. J. Environ. Res. 7: 485-494.

Moussaceb K, Bellache D, Ait-Mokhtar A (2019) Influence of the leaching tests on the release of heavy metals from cementitious materials obtained by the solidification of petroleum sludge wastes. J. Solid Waste Technol. Manag. 45: 139-152.

Pellet M, Laville-Timsit L (1993) Echantillonnage de sols pour caractérisation d'une pollution : Guide méthodologique, BRGM-FRANCE, 16-17: 64-65.

Planel D, Sercombe J, Le Bescop P, Adenot F, Torrenti JM (2006) Long-term performance of cement paste during combined calcium leaching-sulfate attack: kinetics and size effect. Cement Concrete Res. 36: 137-143.

Prasadini P, Lakshmi GS (2014) Environmental science BIRM 301 study material. College of Agriculture, Rajendranagar, p. 4-7.

Rémillard J (2012) Influence de l'altération physique sur les caractéristiques physico-chimiques de monolithes de sols contaminés traités par Stabilisation/Solidification au ciment. Ecole de Technologie Supérieure, University of QUEBEC, p. 25-26.

Qiao X, Poon CS, Cheeseman CR (2007) Investigation into stabilization/solidification performance of Portland cements through cement clinker phases. J. Hazard Mater. 238-243.

Saussaye L, Leleyter L, Baraud F, Boutouil M (2016) Trace and major elements stabilisation in soils treated with hydraulic binders. Eur. J. Environ. Civ. Eng. 22: 755-769.

Sefouhi L, Kalla M, Aouragh L (2010) Trends and problems of municipal solid waste management in Batna City and ň prospects for a sustainable development. Int. J. Sustain. Water Environ. Syst. 1: 15-20.

Segolene R (1992) Arrêté du 18 décembre 1992, stockage de certains déchets industriels spéciaux ultimes et stabilisés pour les installations existantes, 5620.

Shi C, Spence R (2004) Designing of cement-based formula for solidification/stabilization of hazardous, radioactive and mixed wastes. Crit. Rev. Environ. Sci. Tech. 34: 391-417.

Souhila K (2005) Décomposition des matières organiques et stabilisation des métaux lourds dans les sédiments de dragage. Institut national des sciences appliquées de Lyon, France, 74.

Stuart ME, Klinck BL (1998) A catalogue of leachate quality for selected landfills from newly industrialised countries, British Geological Survey, United Kingdom, p. 1-4.

Violaine M (2007) Modifications de la composition de déchets métallifères, miniers et industriels, stabilisés par liants hydrauliques et soumis a des tests de lixiviation, University of Limoge, 79 p.

Windt DL, Badreddine R (2007) Modelling of long-term dynamic leaching tests applied to solidified/stabilized waste. J. Waste Manag. 27: 1638-1647.

Zampori L, Gallo SP, Dotelli G (2009) Long-term leaching test of organo-contaminated cement-clay pastes. J. Hazard. Mater. 170: 1041-1049.

.